Crystal Structure and Physical Properties of Polymorphs of LnAlB₄ (Ln = Yb, Lu)

Robin T. Macaluso,[†,^] Satoru Nakatsuji,[‡,§] Kentaro Kuga,[§] Evan Lyle Thomas,[†]
Yo Machida,[§] Yoshiteru Maeno,[§] Zachary Fisk,[∥] and Julia Y. Chan*,[†]

*Department of Chemistry, Louisiana State University, Baton Rouge, Louisiana 70803, Institute for Solid
State Physics, University of Tokyo, Kashiwa, Japan 277-8581, Department of Physics, Kyoto University,
Kyoto, Japan 606-8502, and Department of Physics and Astronomy, University of California,
Irvine, California 92697-4575*

Single crystals of YbAlB₄ were grown in excess Al flux. Plate- and needle-shaped crystals were found. The plates are found to be β-YbAlB₄, which crystallizes with the ThMoB₄ structure type in space group *Cmmm* (No. 65), $Z = 4$, with lattice parameters of $a = 7.3080(4)$, $b = 9.3150(5)$, and $c = 3.4980(2)$ Å. The needle-shaped crystals were identified as the first form of YbAlB₄ which crystallizes with the YCrB₄ structure type in space group *Pbam* (No. 55), $Z = 4$, with lattice parameters of $a = 5.9220(2)$, $b = 11.4730(3)$, and $c = 3.5060(5)$ Å. While both compounds have heavy fermion ground states with Ising-like magnetic anisotropy, the electronic specific heat coefficients (γ) differ. The β-phase has a γ value near 300 mJ mol⁻¹ K⁻², more than twice that of the α-phase, $\gamma = 130$ mJ mol⁻¹ K⁻². A comparison of the structures and physical properties of both polymorphs is presented.

Introduction

Ytterbium compounds show a wide range of physical properties. Ytterbium can possess either an f^{13} or f^{14} electronic configuration according to Hund's rules; thus, mixed valence behavior has been observed in many Yb-based intermetallic materials, such as Yb₃Pd₄,[1] Yb₃Pt₅,[2] and YbNi₂-Ge₂, YbCu₂Si₂, and YbPd₂Si₂.[3] Magnetic ordering of Yb compounds is rare because the divalent oxidation state of Yb corresponds to a closed shell f^{14} electronic configuration. However, valence fluctuations are possible and have been observed in pnictides of Yb.[4] It is possible to access the Yb²⁺ and Yb³⁺ states as a function of temperature and pressure, in part, due to the small energy difference between Yb²⁺ and Yb³⁺.

Mixed valence behavior is closely associated with heavy-fermion compounds. Most of the known heavy-fermion compounds bear a magnetic moment due to the contribution of *f*-electron density from Ce or U. At low temperatures, the strong coupling between the *f*-electrons and the conduction electrons results in a large electronic effective mass with the electronic specific heat coefficient γ of the order 10² mJ/mol K².[5−7]

Although Yb-based heavy fermion compounds are lacking in the literature, a few have been studied. One example is YbAgCu₄, which is a member of the YbMCu₄ series where the M site can be replaced by a variety of transition metals, including Ag, Au, and Zn.[8] YbAgCu₄ is a moderate heavy-fermion compound with $\gamma > 200$ mJ mol⁻¹ K⁻² and shows no magnetic ordering; in YbAuCu₄, RKKY interactions dominate long-range ordering below 1 K. For M = Zn, no magnetic ordering has been observed above 300 mK. A qualitative comparison of the physical properties leads to the conclusion that M elements with more electrons favor Yb²⁺ while M elements with fewer electrons favor Yb³⁺. Another example is YbRh₂Si₂, for which non-Fermi-liquid behavior has been recently found. Although weak antiferromagnetic order occurs at 65 mK,[9] the magnetic specific heat divided by temperature, C_M/T, reaches a gigantic value, ~1000 mJ mol⁻¹ K⁻², at low temperature. Weak two-dimensional antiferromagnetic fluctuations are most likely the cause of the non-Fermi liquid behavior.[10]

* Corresponding author. E-mail: jchan@lsu.edu.
† Louisiana State University.
^ Current address: School of Chemistry, Earth Science, and Physics, University of Northern Colorado, Greeley, CO 80639.
‡ University of Tokyo.
§ Kyoto University.
∥ University of California, Irvine.

(1) Politt, B.; Durkop, D.; Weidner, P. *J. Magn. Magn. Mater.* **1985**, *47−48*, 583−585.
(2) Oster, F.; Politt, B.; Braun, E.; Schmidt, H.; Langen, J.; Lossau, N. *J. Magn. Magn. Mater.* **1987**, *63−4*, 629−631.
(3) Rao, C. N. R.; Sarma, D. D.; Sarode, P. R.; Sampathkumaran, E. V.; Gupta, L. C.; Vijayaraghavan, R. *Chem. Phys. Lett.* **1980**, *76*, 413−415.
(4) Tateiwa, N.; Kobayashi, T. C.; Amaya, K.; Li, D. X.; Shiokawa, Y.; Suzuki, T. *J. Phys. Soc. Jpn.* **2002**, *71*, 1365−1369.

(5) Fisk, Z.; Ott, H. R.; Rice, T. M.; Smith, J. L. *Science* **1986**, *320*, 124-129.
(6) Fisk, Z.; Hess, D. W.; Pethick, C. J.; Pines, D.; Smith, J. L.; Thompson, J. D.; Willis, J. O. *Science* **1988**, *239*, 33−42.
(7) Fisk, Z.; Sarrao, J. L.; Smith, J. L.; Thompson, J. D. *Proc. Natl. Acad. Sci. U.S.A.* **1995**, *92*, 6663−6667.
(8) Sarrao, J. L.; Immer, C. D.; Fisk, Z.; Booth, C. H.; Figueroa, E.; Lawrence, J. M.; Modler, R.; Cornelius, A. L.; Hundley, M. F.; Kwei, G. H.; Thompson, J. D.; Bridges, F. *Phys. Rev. B* **1999**, *59*, 6855−6866.
(9) Trovarelli, O.; Geibel, S.; Mederle, S.; Langhammer, C.; Grosche, F. M.; Gegenwart, P.; Lang, M.; Sparn, G.; Steglich, F. *Phys. Rev. Lett.* **2000**, *85*, 626−629.
(10) Gegenwart, P.; Custers, J.; Geibel, C.; Neumaier, K.; Tayama, T.; Tenya, K.; Trovarelli, O.; Steglich, F. *Phys. Rev. Lett.* **2002**, *89* 056402/1−4.

Table 1. Crystallographic Parameters of α-LnAlB₄ and β-LnAlB₄ (Ln = Yb, Lu)

formula	α-YbAlB₄	β-YbAlB₄	α-LuAlB₄	β-LuAlB₄
		Crystal Data		
structure type	YCrB₄	ThMoB₄	YCrB₄	ThMoB₄
a (Å)	5.9220(2)	7.3080(4)	5.90500(10)	7.2890(3)
b (Å)	11.4730(3)	9.3150(5)	11.4440(2)	9.2860(5)
c (Å)	3.5060(5)	3.4980(2)	3.5100(4)	3.5040(2)
V (Å³)	238.21(4)	238.12(2)	237.19(3)	237.17(2)
Z	4	4	4	4
crystal dimensions (mm³)	0.05 × 0.05 × 0.05	0.02 × 0.02 × 0.06	0.02 × 0.04 × 0.05	0.01 × 0.02 × 0.08
temperature (K)	298(2)	298(2)	298(2)	298(2)
crystal system	orthorhombic	orthorhombic	orthorhombic	orthorhombic
space group	*Pbam* (No. 55)	*Cmmm* (No. 65)	*Pbam* (No. 55)	*Cmmm* (No. 65)
θ range (deg)	2.55−34.97	2.55−30.02	2.55−30.03	2.55−30.03
μ (mm⁻¹)	29.414	29.815	41.578	41.583
		Data Collection		
measured reflections	3856	2956	2893	1643
independent reflections	591	228	397	351
reflections with $I > 2\sigma(I)$	519	228	378	228
R_{int}	0.0346	0.0387	0.0414	0.0459
h	−8 → 9	−9 → 10	−8 → 8	−9 → 10
k	−18 → 18	−10 → 12	−15 → 15	−12 → 12
l	−5 → 5	−4 → 4	−4 → 4	−4 → 4
		Refinement		
$R(F)$ for $F_o^2 > 2\sigma(F_o^2)^a$	0.0530	0.0568	0.0249	0.0410
$R_w(F_o^2)^b$	0.1368	0.1227	0.0624	0.0986
reflections	446	228	397	225
parameters	38	20	38	20
$\Delta\rho_{max}$ (e Å⁻³)	3.007	6.077	3.019	4.599
$\Delta\rho_{min}$ (e Å⁻³)	−3.143	−10.553	−3.044	−6.367
extinction coefficient	0.037(4)	0.032(4)	0.065(3)	0.025(3)
T_{min}, T_{max}	0.3210, 0.3210	0.2678, 0.5870	0.2303, 0.4902	0.1465, 0.6812

$^a R = \Sigma||F_o| - |F_c||/\Sigma|F_o|$. $^b R_w = [\Sigma[w(F_o^2 - F_c^2)^2]/\Sigma[w(F_o^2)^2]]^{1/2}$.

It has been previously reported that YbAlB₄, like other Yb-based compounds, displays mixed valence behavior.[11] We have found that there are actually two polymorphs of YbAlB₄. To our knowledge, this is the first time that the second polymorph, to which we will refer to as β-YbAlB₄, has been synthesized and characterized. In this paper, we report on the single-crystal growth and structural characterization of the α- and β-forms of YbAlB₄. Our magnetic and thermal measurements reveal that both α-YbAlB₄ and β-YbAlB₄ exhibit a heavy fermion ground state with no magnetic order at least down to 350 mK. Interestingly, the γ value of β-YbAlB₄ is large, ∼300 mJ mol⁻¹ K⁻² at 350 mK, which is more than twice lager than the γ ∼100 mJ/(mol of Yb)·K² for α-YbAlB₄.

Experimental Section

Synthesis. Single crystals of LnAlB₄ (Ln = Yb, Lu) were grown from Al flux. The stoichiometric ratio of Ln:4B was heated in excess Al in an alumina crucible under an Ar atmosphere to 1723 K and then slowly cooled to 1273 K at 5 K h⁻¹. At 1273 K, the furnace was switched off, and the sample was allowed to cool to room temperature. The crucible was then removed from the furnace. After the excess Al flux was etched using a NaOH solution, a mixture of both needle- and platelike crystals were found.

Chemical compositions of single crystals were determined by a scanning electron microscope (SEM, JEOL JSM5600) equipped with energy-dispersive X-ray spectroscopy (EDS, Oxford LINK ISIS) at ISSP, and the analysis of both polymorphs are in good agreement with the ideal compositions of YbAlB₄ within the error.

We also note that our preliminary measurements of the resistivity indicate that the residual resistivity ratios (RRR) of both polymorphs are on the order of 100, which suggests that crystals are of good quality. One explanation for the presence of two polymorphs at the synthesis temperature is that if the temperature was quickly ramped up to 1873 K, more of the alpha phase crystals would be synthesized, in comparison with the heat treatment at 1673 K. This suggests that the alpha phase would be the high-temperature phase. Given that these phases are grown in flux, transformation from one polymorph to the other is also possible during cooling.

X-ray Diffraction. Silver-colored fragments of the needle-shaped α-YbAlB₄ single crystal with dimensions of 0.05 × 0.05 × 0.05 mm³ and the platelike β-YbAlB₄ crystal with dimensions of 0.06 × 0.02 × 0.02 mm³ were mounted on glass fibers with epoxy and aligned on a Nonius Kappa CCD X-ray diffractometer separately. Intensity measurements were performed using graphite monochromated Mo Kα radiation (λ = 0.71073 Å). Data were collected at 298 K. Crystallographic parameters for α- and β-LnAlB₄ (Ln = Yb, Lu) are given in Table 1. Unmerged data were treated with a semiempirical absorption correction by SORTAV.[12] The structural model was refined using SHELXL97.[13] To correct the data, an extinction coefficient was determined from the least-squares cycles and the atomic positions were refined with anisotropic displacement parameters. Similar procedures were followed for the LuAlB₄ needle- and plate-shaped crystals. Atomic positions and displacement parameters for α- and β-LnAlB₄ (Ln = Yb, Lu) are provided in Tables 2a and 2b, and selected interatomic distances and bond angles for α- and β-YbAlB₄ are listed in Table 3.

Physical Property Measurements. The temperature dependence of the magnetic susceptibility has been measured using a Quantum Design SQUID magnetometer in a field of 0.1 T along both the

(11) Fisk, Z.; Yang, K. N.; Maple, M. B.; Ott, H. R. In *Valence Fluctuations in Solids*; Falicov, L. M., Hanke, W., Maple, M. P., Eds.; North-Holland Publishing Company: New York, 1981; pp 345−347.

(12) Blessing, R. H. *Acta Crystallogr.* **1995**, *A51*, 33.
(13) Sheldrick, G. M. *SHELXL97*; University of Göttingen: Göttingen, Germany, 1997.

Table 2. Atomic Positions and Displacement Parameters in Polymorphs

(a) YbAlB$_4$ Polymorphs

atom	Wyckoff position	x	y	z	$U_{eq}{}^a$
			α-YbAlB$_4$		
Yb	4g	0.12940(5)	0.15043(3)	0	0.0055(3)
Al	4g	0.1387(4)	0.4096(3)	0	0.0050(6)
B1	4h	0.2893(18)	0.3126(9)	$^1/_2$	0.0063(16)
B2	4h	0.3659(18)	0.4701(12)	$^1/_2$	0.006(2)
B3	4h	0.384(2)	0.0468(11)	$^1/_2$	0.010(2)
B4	4h	0.474(2)	0.1943(10)	$^1/_2$	0.0087(18)
			β-YbAlB$_4$		
Yb	4i	0	0.30059(5)	0	0.0055(3)
Al	4g	0.1816(8)	0	0	0.0063(10)
B1	4h	0.124(3)	$^1/_2$	$^1/_2$	0.004(3)
B2	8q	0.2232(16)	0.1609(19)	$^1/_2$	0.006(2)
B3	4j	0	0.092(2)	$^1/_2$	0.005(3)

(b) LuAlB$_4$ Polymorphs

atom	Wyckoff position	x	y	z	$U_{eq}{}^a$
			α-LuAlB$_4$		
Lu	4g	0.12981(4)	0.15028(2)	0	0.0053(2)
Al	4g	0.1382(3)	0.4100(2)	0	0.0058(5)
B1	4h	0.2904(13)	0.3131(7)	$^1/_2$	0.0060(14)
B2	4h	0.3683(12)	0.4697(9)	$^1/_2$	0.0076(18)
B3	4h	0.3862(14)	0.0478(7)	$^1/_2$	0.0075(19)
B4	4h	0.4737(13)	0.1932(8)	$^1/_2$	0.0071(14)
			β-LuAlB$_4$		
Lu	4i	0	0.30040(5)	0	0.0038(4)
Al	4g	0.1802(6)	0	0	0.0038(9)
B1	4h	0.120(2)	$^1/_2$	$^1/_2$	0.006(3)
B2	8q	0.2225(14)	0.1597(15)	$^1/_2$	0.0038(17)
B3	4j	0	0.0906(18)	$^1/_2$	0.006(3)

^{a} U_{eq} is defined as one-third of the orthogonalized U_{ij} tensor.

ab-plane and the *c*-axis. The temperature dependence of the specific heat was measured by a thermal relaxation method in zero magnetic field.

Results and Discussion

Crystal Structure. The needle- and platelike morphologies correspond to two different crystal structures. The previously reported crystal structure of YbAlB$_4$[14] is isostructural to YCrB$_4$ and corresponds to our needle-shaped crystals, which we refer to as α-YbAlB$_4$.[15] α-LnAlB$_4$ (Ln = Yb, Lu) forms in the orthorhombic *Pbam* space group, Z = 4, with lattice parameters of a = 5.9220(2), b = 11.4730-(3), and c = 3.5060(5) Å for α-YbAlB$_4$ and a = 5.90500-(10), b = 11.4730(3), and c = 3.5100(4) Å for α-LuAlB$_4$. The plate-shaped crystals form a second polymorph, or β-LnAlB$_4$ (Ln = Yb, Lu), which is isostructural to Th-MoB$_4$.[16] The crystal structure of β-LnAlB$_4$ (Ln = Yb, Lu) is shown in Figure 1. β-LnAlB$_4$ (Ln = Yb, Lu) adopts the orthorhombic structure in the *Cmmm* space group, Z = 4, with lattice parameters of a = 7.3080(4), b = 9.3150(5), and c = 3.4980(2) Å and a = 7.2890(3), b = 9.3150(5), and c = 3.5040(2) Å for β-YbAlB$_4$ and β-LuAlB$_4$, respectively. In both polymorphs of YbAlB$_4$, the Yb and Al atoms reside within the same *ab*-plane and are sandwiched between two B layers. Boron layers have been found in various

(14) Mikhalenko, S. I.; Kuz'ma, Y. B.; Korsukova, M. M.; Gurin, V. N. *Izv. Akad. Nauk SSSR Neorg. Mater.* **1980**, *16*, 1941−1944.
(15) Kuz'ma, Y. B. *Kristallografiya* **1970**, *15*, 372−374.
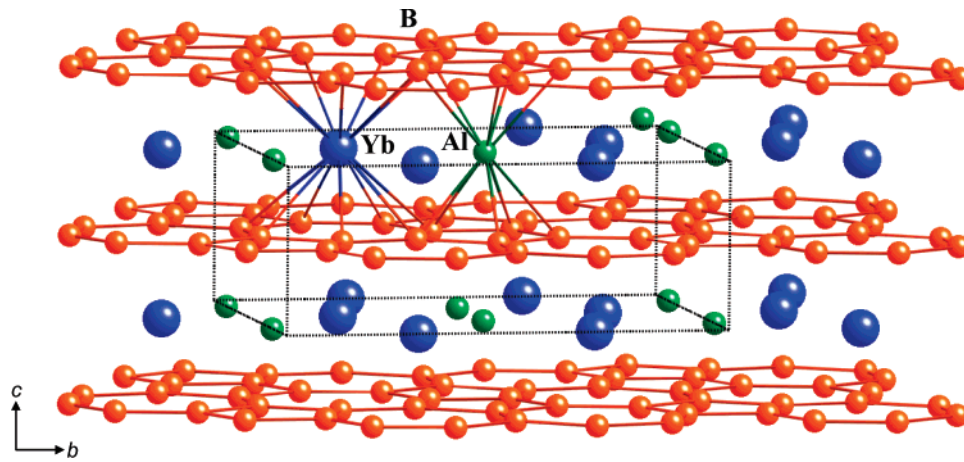(16) Rogl, P.; Nowotny, H. *Monatsh. Chem.* **1974**, *105*, 1082−1098.

Table 3. Selected Interatomic Bond Distances (Å) in YbAlB$_4$

	β-YbAlB$_4$		
	In Boron Layer		
B1−B1	1.82(4)	B2−B3	1.754(16)
B1−B2	1.87(2)	B3−B3	1.71(4)
B2−B2	1.71(4)		
	In Yb/Al Layer		
Yb−B1 (×4)	2.708(7)	Al−B1 (×4)	2.253(13)
Yb−B2 (×4)	2.723(11)	Al−B2 (×2)	2.323(12)
(×4)	2.698(9)	Al−B3 (×4)	2.356(8)
Yb−B3 (×2)	2.616(14)		
	α-YbAlB$_4$		
	In Boron Layer		
B1−B2	1.863(18)	B2−B2	1.73(2)
B1−B4	1.74(2)	B2−B3	1.723(14)
	1.867(18)	B3−B3	1.74(3)
		B3−B4	1.774(17)
	In Yb/Al Layer		
Yb−B1 (×2)	2.704(8)	Al−B1 (×2)	2.260(7)
(×2)	2.726(9)	Al−B2 (×2)	2.316(7)
Yb−B2 (×2)	2.712(10)	Al−B3 (×2)	2.361(9)
(×2)	2.724(9)	Al−B3 (×2)	2.365(9)
Yb−B3 (×2)	2.600(10)	Al−B4 (×2)	2.332(9)
Yb−B4 (×2)	2.663(9)		
(×2)	2.738(9)		

extended structures including the hexagonal layers in the AlB$_2$ structure type[17] and layers of hexagons and disordered triangles stacked along the *c*-axis of Be$_{1.09}$B$_3$.[18]

The boron layers along the *ab*-plane in α- and β-YbAlB$_4$ are shown in Figures 2a and 2b, respectively. The layers, which can be viewed as two-dimensional networks of boron in heptagonal and pentagonal rings, have been compared and

Figure 1. Layers of β-YbAlB₄. Boron, shown as orange spheres, forms two-dimensional sheets along the *ab*-plane. Layers of Yb, shown in blue, and Al, shown in green, are interleaved between the B layers. Dashed lines show the orthorhombic unit cell. Some interlayer bonding has been omitted for clarity.
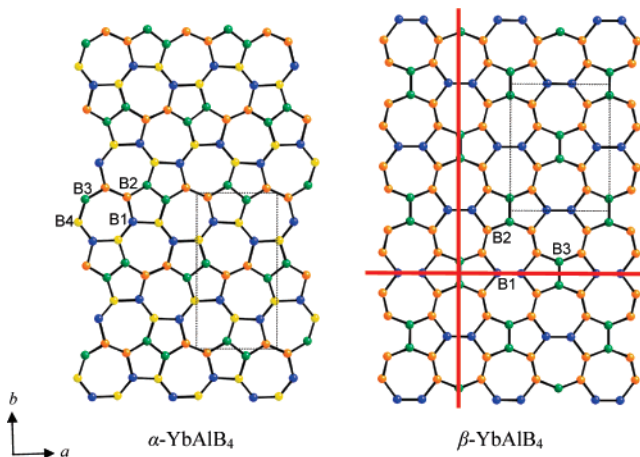

Figure 2. Boron layers along [020] for (a) α-YbAlB₄ and (b) β-YbAlB₄. The unit cell is outlined with grey lines. For α-YbAlB₄, the B1, B2, B3, and B4 atoms are shown as blue, orange, green, and yellow spheres, respectively. For β-YbAlB₄, the B1, B2, and B3 atoms are shown as blue, orange, and green spheres, respectively. Mirror planes are depicted as solid red lines.

Figure 3. Temperature dependence of the magnetic susceptibility for α-YbAlB₄ (open symbols) and β-YbAlB₄ (solid symbols). The *ab*-plane data are shown in circles with the *c*-axis data in squares.

related to similar structures.[19] In α- and β-YbAlB₄, the B–B interatomic distances within the *ab*-plane are 1.74(2) and 1.867(18) Å, similar to the average homoatomic bonding distance of 1.796(28) Å in alpha, tetragonal, and rhombohedral polymorphs of boron.[20]

Although the packing arrangements within the B layers distinguish the two polymorphs, the Yb/Al layers are quite similar. In both structures, Yb atoms are centered between two heptagonal rings, and Al is centered between two pentagonal rings. For β-YbAlB₄, Yb–B distances range between 2.616(14) and 2.723(11) Å, and Al–B interatomic distances are between 2.253(13) and 2.356(8) Å, whereas in α-YbAlB₄, Yb and B are separated by 2.600(10)–2.738-(9) Å and Al and B by 2.260(7)–2.365(9) Å. These distances are suggestive of bonding according to the sum of the atomic radii of Yb (1.74 Å), Al (1.43 Å), and B (0.98 Å);[21] thus,
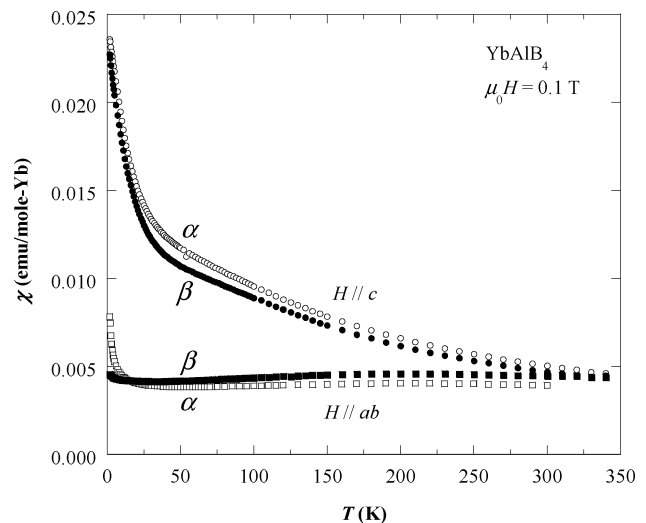
Yb most likely bears a valence of 3+. For both the α- and β-polymorphs, the Yb–Yb distance is shortest for that along the *c*-axis, which is given by the *c*-axis parameter of $\sim$3.5 Å. This is also the distance between the B layers. On the other hand, Yb–Yb distances in the *ab*-plane are 3.740 and 3.777 Å for α-YbAlB₄ and 3.715 and 3.772 Å for β-YbAlB₄. Yb and Al atoms are separated by 2.974 and 3.094 Å for the α-phase and by 2.977 and 3.099 Å for the β-phase, similar to bonding distances of $\sim$2.97 and $\sim$3.27 Å in YbAl₂[22] and YbAl₃,[23] respectively.

Figure 3 shows the temperature dependence of the susceptibility for both α- and β-YbAlB₄. Both exhibit nearly the same temperature dependence. Interesting to note for these materials is the strong Ising anisotropy along the *c*-axis. The Curie–Weiss fit to the *c*-axis component above 100 K yields effective moments of $p_{eff}^c = 5.01(5)$ μ_B/Yb for the α-phase and $p_{eff}^c = 4.96(5)$ μ_B/Yb for the β-phase, indicating a Yb³⁺ state as expected for the high-temperature state of

(17) Hofmann, W.; Janiche, W. *Z. Phys. Chem. B* **1936**, *31*, 214–222.
(18) Macaluso, R. T.; Sarrao, J. L.; Pagliuso, P. G.; Moreno, N. O.; Goodrich, R. G.; Browne, D. A.; Fronczek, F. R.; Chan, J. Y. *J. Solid State Chem.* **2002**, *166*, 245–250.
(19) Deza, M.; Fowler, P. W.; Shtogrin, M.; Vietze, K. *J. Chem. Inf. Comput. Sci.* **2000**, *40*, 1325–1332.
(20) Donohue, J. *The Structures of the Elements*; John Wiley & Sons: New York, 1974.

(21) Emsley, J. *The Elements*, 2nd ed.; Oxford University Press: New York, 1991.
(22) Palenzona, A. *J. Less-Common Met.* **1972**, *29*, 289–292.
(23) Havinga, E. E.; Buschow, K. H. J.; Vandaal, H. J. *Solid State Commun.* **1973**, *13*, 621–627.
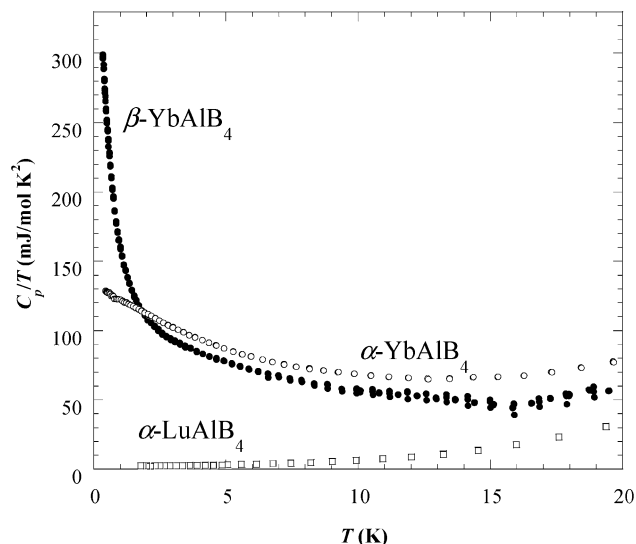
Figure 4. Temperature dependence of the specific heat divided by temperature, C_p/T for α-YbAlB$_4$ (open circles), β-YbAlB$_4$ (solid circles), and α-LuAlB$_4$ (open squares).

the intermediate valence systems. On the other hand, the spatial average of the effective moments $(2(p_{eff}^{ab})^2 + (p_{eff}^c)^2)^{1/2}$ is about 2.9 μ_B/Yb for both phases, and much smaller than 4.53 μ_B/Yb, the expected value for $J = {}^7/_2$ full multiplet of Yb^{3+}. This suggests a strong crystal field effect due to the low spatial symmetry at the Yb sites. Generally, for the Kondo lattice systems, the Weiss temperatures (θ) give roughly the square root of 2 times the Kondo temperature,[24] and θ values are found $-190(9)$ K for the α-phase and $-195(9)$ K for the β-phase. Thus, for these systems, the Kondo temperature is roughly the same, ∼130 K, a typical value for intermediate valence systems.

Figure 4 shows the temperature dependence of the specific heat divided by temperature, C_p/T for both α- and β-YbAlB$_4$.

(24) Nakatsuji, S.; Yeo, S.; Balicas, L.; Fisk, Z.; Schlottmann, P.; Pagliuso, P. G.; Moreno, N. O.; Sarrao, J. L.; Thompson, J. D. *Phys. Rev. Lett.* **2002**, *89*, 106402.

In comparison with these results, C_p/T for both LuAlB$_4$ phases is small (below 20 K), as can be typically seen for the data of α- LuAlB$_4$ in Figure 4. No nuclear contribution from Yb, Al, and B is expected above 0.35 K. Furthermore, no anomaly due to the magnetic ordering is found, and thus, the data in Figure 4 should represent the electronic contribution. Notably, the C_p/T for both polymorphs starts increasing below ∼10 K, indicating the heavy fermion formation at low temperatures. On further cooling, the C_p/T for the α-phase increases and saturates near 130 mJ mol^{-1} K^{-2}, whereas C_p/T for the β-phase increases more rapidly on cooling, reaching 300 mJ mol^{-1} K^{-2} at 0.35 K (the lowest temperature measured). The integration of C_p/T up to 20 K yields the entropy of approximately 1400 mJ mol^{-1} K^{-2}, less than one-fourth of R ln 2. This indicates that the ground states of both the α- and β-phases are most likely heavy fermion states based on a ground-state doublet. The enhancement of the electronic specific heat coefficient γ in the β-phase relative to that of the α-phase is interesting and may be related to the higher symmetry of the crystal structure of the β-phase. We plan to perform further detailed measurements to reveal the relationship between the structures and the physical properties.

Supporting Information Available: Additional information in CIF format. This material is available free of charge via the Internet at http://pubs.acs.org.

CM062244+